DOI 10.59887/2073-6673.2023.16(3)-7

УДК 627.52

© *I. G. Kantarzhi*[1*], *I. O. Leont'ev*[2], *A. V. Kuprin*[1,] 2023
© Translation from Russian: *E. S. Kochetkova*, 2023
[1]Moscow State University of Civil Engineering (National Research University) (MSUCE), 26 Yaroslavl highway, Moscow, 129337, Russia
[2]Shirshov Institute of Oceanology, Russian Academy of Sciences, 36 Nakhimovsky Prosp., Moscow 117997, Russia
*kantardgi@yandex.ru

ANALYTICAL STUDIES OF THE DYNAMICS OF POCKET BEACH

Received 22.02.2023, Revised 01.06.2023, Accepted 24.07.2023

Abstract

The beach site is located in the utmost northeastern part of the Nevskaya Bay. A boulder dam is built on the western side, which, however, fails to protect the beach from the effects of waves that cause longshore sediment transport. The planned construction of transverse beach-retaining structures outlines in the "Water Sports Base in Primorsky District" initiative, might change the current situation. This study objective is to predict the evolution of the coastal contour resulting from the planned construction in the next few decades. A natural analogue of such an artificial structure could be a pocket beach located between two natural promontories. The sediment equilibrium at this study location includes three main components: volumes of erosion, accumulation and bypassing. The results include the computed wave patterns and the movement of sediment along the shoreline. The lateral sediment transport diminishes notably over time, driven by the alteration of the shoreline contour and the reduction in the angle between the wave equilibrium and the coastal resultant. The erosion and accumulation volumes increase over time, but their rates slow down. The shoreline displacement becomes more prominent over time; however, the rates of erosion differ from accumulation. The shoreline is moving particularly fast in the first years after construction, and then the process slows down gradually. The introduction of artificial beach protection structures in the 300th Anniversary Park of St. Petersburg will considerably reduce both the pace of beach erosion and the affected area. However, the erosion process will not be completely halted.

Keywords: pocket beach, longshore sediment transport, shore evolution, accumulation, bypassing, shore protection

© *И. Г. Кантаржи*[1*], *И. О. Леонтьев*[2], *А.В. Куприн*[1], 2023
© Перевод с русского: *Е.С. Кочеткова*, 2023
[1]Национальный исследовательский Московский государственный строительный университет, 129337, Москва, Ярославское шоссе, д. 26.
[2]Институт океанологии им. П.П. Ширшова РАН, 117997, Москва, Нахимовский проспект, д. 36.
*kantardgi@yandex.ru

АНАЛИТИЧЕСКИЕ ИССЛЕДОВАНИЯ ДИНАМИКИ «КАРМАННОГО ПЛЯЖА»

Статья поступила в редакцию 22.02.2023, после доработки 01.06.2023, принята в печать 24.07.2023

Аннотация

Исследуется динамика пляжа, расположенного между естественными или искусственными поперечными преградами. Рассматривается пляж, расположенный в северо-восточной части Невской губы Финского залива. В западной части пляжа располагается валунная дамба, которая, однако, не обеспечивает защиту пляжа от размыва, вызванного вдольбереговым переносом наносов. Для обеспечения устойчивости пляжа в рамках проекта «База водных видов спорта в Приморском районе» планируется построить поперечные пляжеудерживающие сооружения. Целью данной работы является прогнозирование динамики береговых процессов рассматриваемого пляжа в новых условиях на срок ближайших двадцати лет. Рассчитан баланс наносов, который для рассматриваемого карманного пляжа состоит из трёх составляющих: объем эрозии, объём аккумуляции и объём байпассинга. По результатам расчетов выяснено, что в новых условиях вдольбереговой поток наносов со временем заметно уменьшается, что обусловлено разворотом контура берега и уменьшением угла волновой равнодействующей

Ссылка для цитирования: *Кантаржи И.Г.*, *Леонтьев И.О.*, *Куприн А.В.* Аналитические исследования динамики «карманного пляжа» // Фундаментальная и прикладная гидрофизика. 2023. Т. 16, № 3. С. 93–105. doi:10.59887/2073-6673.2023.16(3)-7
For citation: *Kantarzhi I.G.*, *Leont'ev I.O.*, *Kuprin A.V.* Analytical Studies of the Dynamics of Pocket Beach. *Fundamental and Applied Hydrophysics*. 2023, 16, 3, 93–105. doi:10.59887/2073-6673.2023.16(3)-7

относительно береговой нормали. Было получено, что процессы размыва и аккумуляции в новых условиях со временем замедляются. Выдвижение берега в первые годы после строительства демонстрирует высокую скорость, замедляясь со временем. Отступание берега происходит более равномерно, также со временем замедляясь. Строительство рассматриваемых пляжеудерживающих сооружений позволяет замедлить процессы размыва береговой части «Парка 300-летия Санкт-Петербурга», однако данных мер недостаточно для полной остановки процесса размыва.

Ключевые слова: карманный пляж, вдольбереговой перенос наносов, эволюция берега, аккумуляция, байпассинг, берегозащита

1. Introduction

The beach in question is located in the extreme northeastern part of the Neva Bay. On the western side, there is a boulder dam (essentially a groyne), which, however, does not protect the beach from the effects of waves responsible for alongshore sediment transport (Fig. 1) [1]. Since the beach has boundary on the eastern side, the material is carried out beyond its limits, and the coast recedes rather quickly. The distance between the calm line and the retaining wall of the embankment surrounding the beach has decreased significantly in recent years, which creates a threat of destruction during storm surges.

The planned construction of transverse beach-retaining structures outlined in the project "Water Sports Base in the Primorsky District" (hereinafter 'groynes') may alleviate the current situation. The most crucial role in this will be attributed to groyne #3, which will delimit the beach from the eastern side and prevent material erosion (see Fig. 1). The shift in sediment balance will evidently lead to a significant morphological reshaping of the coastline. The objective of this study is to predict the evolution of the shoreline contour under the new conditions for the upcoming decades.

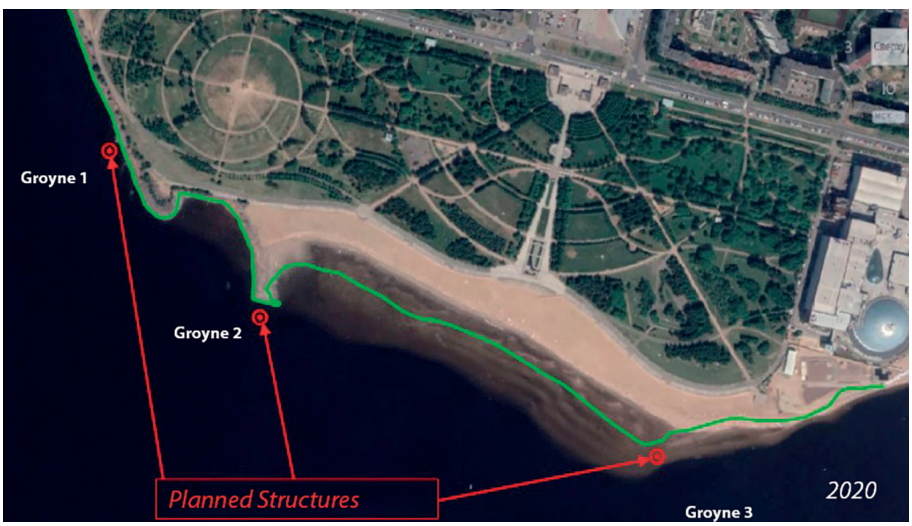

Fig. 1. Modern image of the beach. The green line shows the water's edge in 2009

In the framework of this study an analysis was conducted on prior research pertaining to the subject. The study did not aim for a deep analysis of the impact of transverse structures on the adjacent beach dynamics. The topic has been extensively covered, including a review in Leontyev I.O.'s book [2]. Interactions between waves, structures, and sedimentation are described in Hanson H. [3,4]. Numerical modeling is used for shoreline protection from waves, as shown in Kantarzhi I.G. et al.'s work [5]. Articles [6,7] discuss a predictive model for shoreline changes resulting from common coastal structures like groynes, breakwaters, and harbor jetties. Additionally, [8] considers a combined approach of modeling and monitoring to assess the impact of designed coastal protective structures on shoreline processes.

2. Materials and Methods

A natural analogue to such a contemplated artificial feature can be the so-called pocket beach, situated between two natural headlands or artificial transverse barriers (see Fig. 2).

Fig. 2. Cleopatra's Beach, Turkey, Aegean Sea

Pocket beaches are small beaches that form between promontories and within bays along rocky coastlines. They are composed of a mixture of boulders, pebbles, sand, and silt, exhibiting a combination of shoreline types. Their evolution is influenced by wave action and morphological characteristics. The most commonly observed dynamics is beach rotation based on the prevailing wave direction [9].

The morphological evolution of these systems is determined by wave conditions, which influence both coastal hydrodynamics [10] and beach formation processes. It is also known that the morphological behavior of these beaches is influenced by the beach shape, type and slope of the beach face, grain size of the beach-forming material, and the presence or absence of nearshore shoals.

Pocket beaches can be extremely sensitive to low-frequency or high-energy storm events, as demonstrated by some beaches on Elba Island [11]. Pocket beaches are often fed by small streams characterized by low sediment discharge rates. Beach deposits from local streams in bays are frequently coarse and unsorted [12], and they exist in shoreline deposits that cannot be eroded by available wave energy [13].

Their distinct feature lies in the fact that over time, the shoreline aligns itself perpendicular to the direction of the resultant wave action. As a result, alongshore movements in opposite directions compensate for each other, ensuring the stability of the coast.

Evidently, in the case of an artificial pocket beach, its evolution will follow the same path. If the resultant wave direction is angled Θ_R relative to the shoreline normal, its contour will gradually adjust to reduce this angle over time, leading to a diminishing resultant alongshore transport (see Fig. 3). As shown in Fig. 3, the total beach length, as well as the sizes of the accretion and erosion areas, are characterized by the values of l, l_{Ac}, and $(l - l_{Ac})$, respectively. The average shoreline displacements in these designated areas are labeled as E and A, while the maximum displacements are denoted as E_m and A_m.

The sediment balance in the considered case involves three main components: erosion volumes (scour) E_r, accretion A_c, and bypassing (material transport around the head of the structure) B_p.

$$Er = Ac + Bp, \tag{1}$$

furthermore, the value of Ac can be expressed as:

$$Ac = Er\left(1 - f_{Bp}\right), \; f_{Bp} = \frac{Bp}{Er}, \tag{2}$$

where f_{Bp} is the bypass coefficient, representing the fraction of material leaving the lithodynamic system.

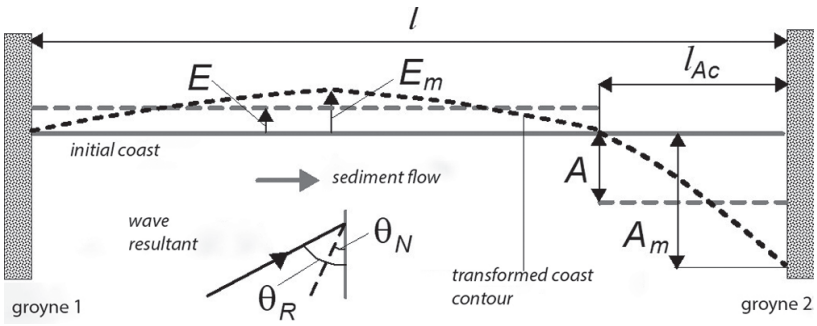

Fig. 3. Contour changes of a shoreline situated between two transverse structures

Let Q_{l0} the annual alongshore sediment flow prior to the construction of groyne 2 (see Fig. 3). The flow Q_l should decrease due to the noted shoreline contour changes in subsequent years, i. e.

$$Q_l = f_\Theta Q_{l0}, \tag{3}$$

where $f_\Theta \le 1$. The value of f_Θ should depend on the rotation angle Θ_N of the shoreline normal with respect to the initial position. As Θ_N approaches Θ_R, the angle of the initial resultant wave direction, the value of f_Θ should tend towards zero. The current value of Θ_N can be estimated based on the achieved maximum shoreline displacements E_m and A_m. This leads to the following relationships:

$$f_\Theta = \frac{\Theta_R - \Theta_N}{\Theta_R}, \ \Theta_N = \mathrm{arctg}\left(\frac{E_m + A_m}{0.5\left(l + l_{Ac}\right)}\right). \tag{4}$$

Further on, we will use the value of $\Theta_R = \Theta_{R*}$ at the depth h_*, marking the seaward boundary of the sediment flow, which will be determined later.

The volume of scour over a time period T, following construction, will be determined as:

$$Er = \int_0^T Q_l dt = Q_{l0} T^*, \ T^* = \int_0^T f_\Theta dt, \tag{5}$$

where $T^* < T$ it makes sense in the context of a virtual time period (at $Q_l = Q_{l0}$ the value of $T^* = T$).

Further, a concept of an active coastal profile is used, defined as a region where sediment fluxes and morphological changes of the seabed are concentrated (see Fig. 4). The active profile is located between the maximum beach elevation z_m and the closure depth h_*, which defines the area of significant storm-induced deformations. Within the profile length l_*, two sections are distinguished, the foreshore with a width of l_b and its submerged portion $l_* - l_b$ (see Fig. 4).

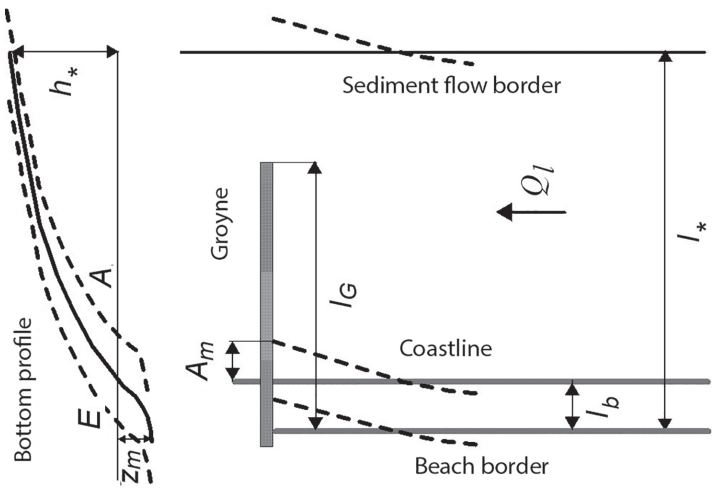

Fig. 4. Parameters of the active coastal profile and its displacement during evolution

It is assumed that the change in the shoreline position is accompanied by the displacement of the entire active shoreline profile as a unified entity [14]. This enables the determination of average shoreline displacements E and A in scour and accretion segments as follows:

$$E = \frac{Er}{(h_* + z_m)(l - l_{Ac})}, \; A = \frac{Ac}{(h_* + z_m) l_{Ac}}. \tag{6}$$

In the initial approximation, the shoreline contour $S(x)$ can be represented as a half-phase sine wave in the scour zone and an inclined straight line in the accretion zone [15]:

$$S(x) = E_m \sin 2\pi \frac{x}{l - l_{Ac}}, \; 0 \le x \le l - l_{Ac}, \; E_m = \frac{\pi}{2} E,$$

$$S(x) = -A_m \frac{x - (l - l_{Ac})}{l_{Ac}}, \; l - l_{Ac} \le x \le l, \; A_m = 2A, \tag{7}$$

where the maximum displacements E_m and A_m are determined from geometric relationships.

The depth h_* in Eq.6 is expressed in terms of the significant wave height H_{s012}, which is exceeded less than 12 hours a year. Furthermore, h_* depends on the specified seabed deformation threshold Δh_c, and at $\Delta h_c = 0.1$m, it can be found from the relationship [24]:

$$h_* = \bar{K} H_{s012}, \; \bar{K} = \left[0.32 \left(\frac{H_0}{L_0} \right)^{-4/15} + 0.99 \left(\frac{H_0}{L_0} \right)^{4/55} \right], \tag{8}$$

where H_0/L_0 the wave steepness (typically $h_* = (1.5 \div 1.6) H_{s012}$).

The extent of the accretion area l_{Ac} is linked to the scale of the structure's influence zone Λ, which depends on both the length of the structure l_G, and the width of the sediment flow l_* [3]:

$$\Lambda = \sqrt{l_* l_G} \;\text{ at }\; l_G \le l_*; \; \Lambda = l_* \;\text{ at }\; l_G > l_*. \tag{9}$$

The length l_G, as well as l_*, is measured from the upper boundary of the beach (marked as z_m, Fig. 4). For a sufficiently extensive beach, the accretion area expands over time t, following the relation $l_{Ac} = \Lambda\sqrt{t}$. However, with a limited beach length, the value of l_{Ac} cannot keep increasing and should stabilize at (1÷2) Λ. In further calculations, it is assumed that

$$l_{Ac} = 1{,}5\Lambda. \tag{10}$$

As the shoreline advances towards the head of groyne 2, the volume of retained material should decrease, while the volume of bypassed material increases. Accordingly, the bypass coefficient f_{Bp} in Eq. 2 can be determined (see Fig. 4):

$$f_{Bp} = \frac{l_* - (l_G - A_m)}{l_*}. \tag{11}$$

Apparently, $f_{Bp} \to 1$ as $A_m \to l_G$. The relationship between the length of the structure l_G and the width of the sediment flow on the submerged slope l_* is of importance also (Fig. 4). Two cases are distinguished here: the case of a short structure, when $l_G \le l_*$, and the case of a long structure, when $l_G > l_*$. In the first case, the relationship (11) is directly applicable. In the second case, it is applicable with an additional condition of $A_m > l_G - l_*$. When $A_m \le l_G - l_*$, the $f_{Bp} = 0$.

Thus, the provided relationships entirely define the considered lithodynamic system.

The basis for wave calculations was provided by long-term wind regime observations at the Neva Port station [16]. For the main wave-hazardous directions, Table 1 has been compiled, showing the frequencies of the most significant situations with wind speeds exceeding 9 m/s.

The frequency refers to the ice-free period (April-December). Also provided are wave fetch lengths and average water depths for the main directions.

Using the recommended formulas [17], average wave parameters were calculated and then converted into significant wave heights H_s and associated wave periods T_s. The obtained results are presented in Table 2. The right-most column indicates the duration of each wave-hazardous situation t_w throughout the year.

Table 1

Initial data on wind

Wind speed, m/s	Repeatability,%		
	S	SW	W
9–10 (9.5)	0.298	1.183	4.329
11–12 (11.5)	0.064	0.207	1.216
13–14 (13.5)		0.049	0.350
15–16 (15.5)		0.012	0.052
17–20 (18.5)			0.018
Acceleration length, km	11	16	22
Average depth, m	2.5	4	4

Table 2

Calculated wave parameters

W, m/s	Direction	$\bar{H}$, m	$\bar{T}$, s	H_s, m	T_s, s	t_w, hour
9.5	S	0.28	2.12	0.45	2.55	19.7
	SW	0.38	2.56	0.60	3.07	78.1
	W	0.39	2.63	0.63	3.15	286
11.5	S	0.32	2.18	0.50	2.61	4.2
	SW	0.43	2.65	0.69	3.18	13.7
	W	0.45	2.71	0.71	3.25	80.3
13.5	S	–	–	–	–	–
	SW	0.48	2.71	0.76	3.26	3.2
	W	0.49	2.76	0.78	3.31	23.1
15.5	S	–	–	–	–	–
	SW	0.52	2.76	0.83	3.31	0.8
	W	0.53	2.80	0.84	3.35	3.4
18.5	S	–	–	–	–	–
	SW	–	–	–	–	–
	W	0.58	2.83	0.92	3.40	1.2

The determination of the wave resultant is based on calculating energy fluxes for the wave-hazardous directions. An elementary energy flux F:

$$F = EC_g \approx 10^3 H^2 T \ \ [\text{J/m/s}], \tag{12}$$

where $E = \frac{1}{8}\rho g H^2$ is the wave energy per unit area, $C_g = \frac{1}{2} gT / 2\pi$ energy transport velocity (wave group velocity), ρ is water density, g is acceleration due to gravity. The meridional component F_{cross} and latitudinal component F_{long} of annual energy fluxes, as well as the azimuth of the wave resultant α_R are determined by the relationships:

$$F_{cross} = \sum_j \sum_i \left(Ft_w\right)_{ij} \cos\alpha_j \,,\ F_{long} = \sum_j \sum_i \left(Ft_w\right)_{ij} \sin\alpha_j \,,\ \tan\alpha_R = \frac{F_{cross}}{F_{long}}, \tag{13}$$

where the indices j and i refer to the specific direction and height (and period) of the waves, respectively.

In this case, the azimuth of the wave resultant is α_R =261°. The azimuth of the observed coastline is close to 300°, and the azimuth of its normal is α_N = 210°. Therefore, the angle of the resultant relative to the coastal normal is $\Theta_R = \alpha_R - \alpha_N$ = 51°.

According to the data in Table 2, the significant wave height is H_{s012} = 0.8m, and the associated period is T_{s012} = 3.3s. Then, according to equation (8), the closure depth is h_* = 1.2m. The calculation of wave refraction for the period T_{s012} yields an angle for the wave resultant at the closure depth of Θ_{R*} = 30°.

Table 3

Longshore sediment fluxes, $10^3 m^3$/year

Rhumb	S	SW	W
Θ_0, deg.	−30	15	60
$\Sigma Q_i t_{wi}$	−0.06 (−0.05))	0.35 (0.28)	2.38 (1.90)
Θ_{net}	2.67 (2.13)		

The alongshore sediment transport rate Q, expressed in cubic meters per hour (m^3/h), can be determined using formula [18]:

$$Q = 0.005\mu_h \left(0.8 + 0.02\frac{\sqrt{gh_B}}{w_g} \right) H_{rmsB}^2 \sqrt{gh_B} \sin\Theta_B \cos\Theta_B , \quad (14)$$

where $\mu_h = 3600\left[\left(\rho_g / \rho - 1 \right)\left(1 - \sigma \right) \right]^{-1}$, ρ_g/ρ is the ratio of solid particle density to water density, σ is the porosity of the sandy soil, g is the acceleration due to gravity, w_g is settling velocity of solid particles (hydraulic size), H_{rmsB} root mean square wave height at the depth of breaking h_B, where the wave approach angle is characterized by the value of Θ_B.

The resultant sediment transport rate Q_{net}

$$Q_{net} = \sum_j \sum_i \left(Q t_w \right)_{ij} , \quad (15)$$

where t_w is the duration of the action of this transport (in hours per year), and the indices i and j correspond to the specific wave height and their direction, respectively.

The sediment transport estimations are presented in Table 3. The calculations were conducted for two characteristic sand sizes on the considered beach 0.3 and 0.4mm (in parentheses). In further calculations, the average flux is set to $2.4 \times 10^3 m^3$/year.

3. Results and Discussion

On average, the scour intensity of the beach is 4.5 meters per year. Therefore, in its natural state, the beach could be completely scoured up to the retaining wall (promenade) within 10 years.

All the initial forecast data are presented in Table 4 [19]. Beach parameters were assessed using characteristic coastal profile (see Fig. 5).

Table 4

Initial parameters for calculations

Θ_{R^*}, deg.	Q_{l0}, 10^3 m^3/year	l, m	h_*, m	z_m, m	l_*, m	l_G, m	Λ, m
30	2.4	600	1.2	2.0	120	120	120

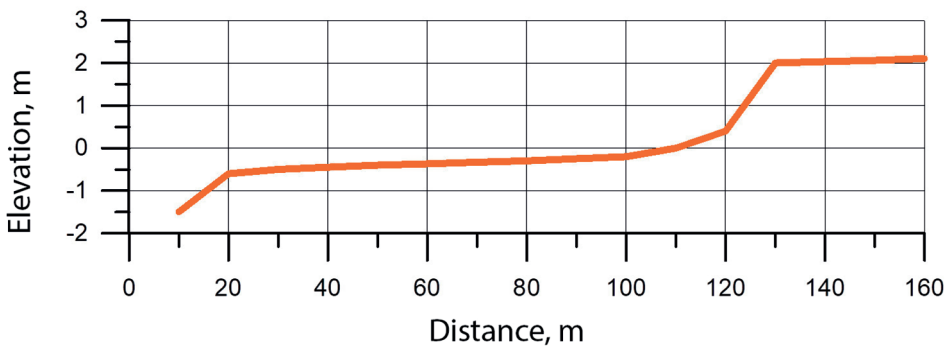

Fig. 5. Typical coastal profile in the study area

The results are shown in Table 5. It reflects the expected changes in important dynamic parameters for the next 20 years. These parameters include the sediment flux along the coast, erosion, deposition, accumulation, and bypassing volumes, and the maximum shifting of the shoreline in erosion and deposition areas. Figures 6, 7, and 8 present the results graphically.

As seen in Fig. 6, the alongshore sediment transport gradually decreases over time. This is due to the changing coastline contour and a reduction in the angle of the wave resultant with respect to the shoreline normal.

Erosion and deposition volumes increase over time, while the rates of erosion and deposition processes slow down (Fig. 7).

Over the course of 20 years, erosion will reach a value of 28 thousand cubic meters, while accumulation near the structure (groyne #3) will be 15.4 thousand cubic meters. Consequently, the material carried away from the beach around the head of the structure (bypassing) will amount to 12.6 thousand cubic meters. Moreover, from Fig. 7, it is evident that the bypassing volume increases almost linearly over time.

As for the shoreline, the displacements increase over time, but the rates of erosion differ from deposition. The shoreline expands particularly rapidly near the structure during the first years after construction. Subsequently, the process gradually slows down, but over the course of 20 years the shore will broaden for more than 50 m.

The retreat of the shoreline in the erosion zone occurs uniformly, it slows down over time. Over the course of 20 years, the shoreline will retreat for 30 meters approximately.

Figure 9 illustrates how the shoreline's shape will change in the next 20–30 years due to the newly built groynes (groynes 2 and 3).

A clockwise rotation of the shoreline is evident, driven by the contour's tendency to reach an equilibrium position relative to the wave resultant. The rate of beach erosion diminishes, and the erosion zone becomes concentrated in the central area between groynes 2 and 3. Complete erosion of this localized beach segment is projected within 20–30 years.

Table 5

Predicted indicators of beach evolution

Years	Sediment flux, 10^3 m^3/year	Erosion volume, 10^3 m^3	Accumulation volume, 10^3 m^3	Bypassing volume, 10^3 m^3	Shore retreat, m	Shore extension, m
1	2.30	2.30	2.17	0.13	2.7	7.5
3	2.09	6.34	5.38	0.96	7.4	18.7
5	1.94	9.84	7.68	2.16	11.5	26.7
7	1.85	13.0	9.45	3.52	15.1	32.8
10	1.70	17.3	11.5	5.66	20.0	39.8
13	1.58	20.8	13.0	7.81	24.3	45.2
15	1.54	23.1	13.8	9.21	26.9	48.1
18	1.44	26.2	14.9	11.3	30.6	51.8
20	1.39	28.0	15.4	12.6	32.7	53.7

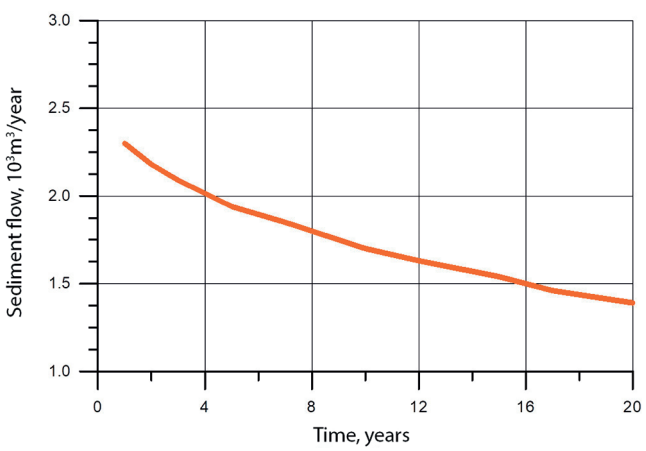

Fig. 6. Predicted changes in longshore sediment flow

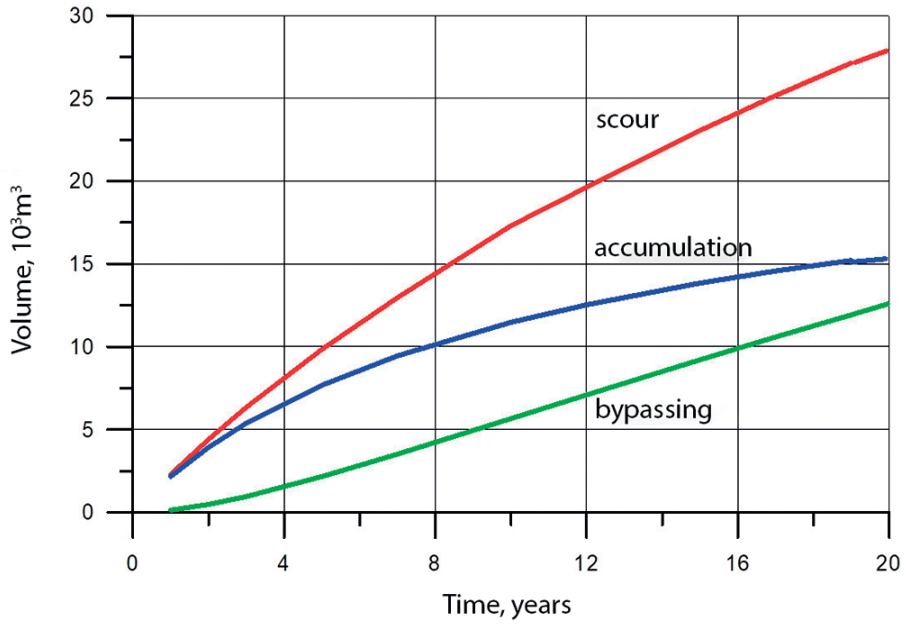

Fig. 7. Predicted scour, accumulation, and bypass volumes

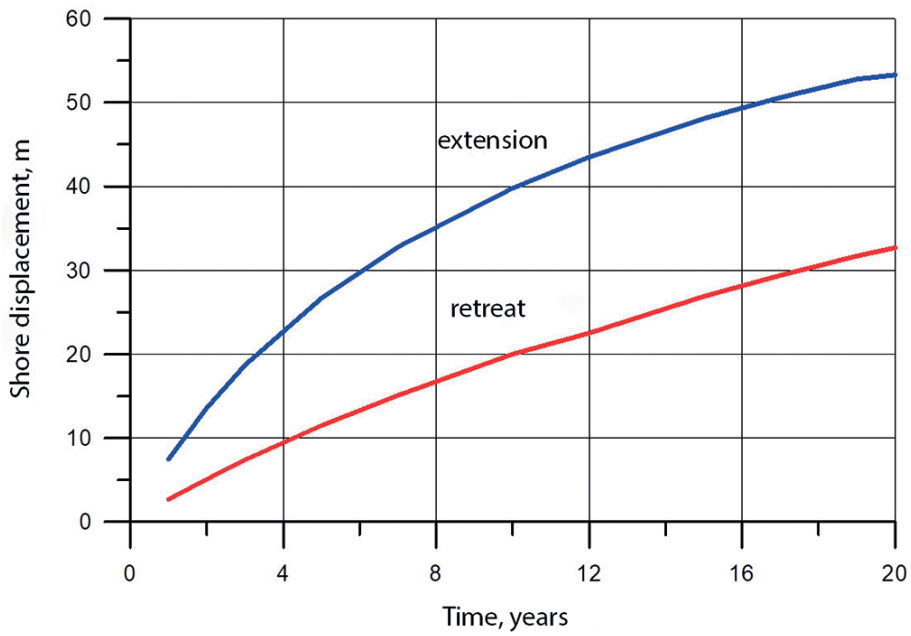

Fig. 8. Maximum shoreline displacements as a function of time

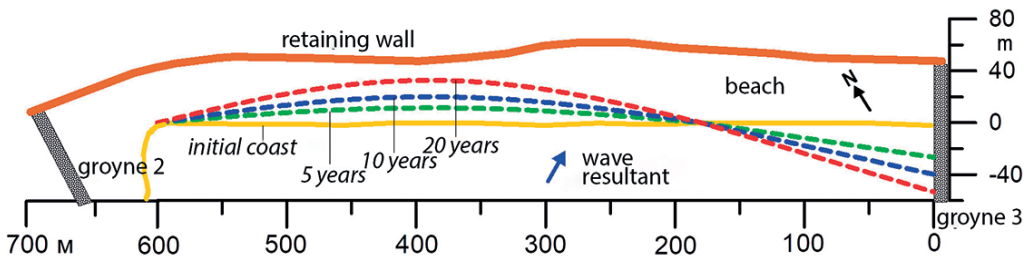

Fig. 9. Expected evolution of the coastal contour

Consequently, the planned structures will significantly slow down the beach erosion process and limit the area of intense erosion, although it will not be able to completely halt the erosion process. Irreversible material loss will decrease notably, simultaneously initiating the process of reshaping the beach contour. This process will involve a local retreat of the shoreline in the central beach area and accumulation of material around groynes 2 and 3.

The construction site is within a seismic zone of magnitude 5, and therefore, the depth and intensity of erosion can be influenced by soil liquefaction, which might occur due to increased pore pressure during seismic loads in the soil. There are two types of soil liquefaction mechanisms on the seabed: instantaneous liquefaction and residual liquefaction [20]. Instantaneous liquefaction can only occur in very dense sand. Its impact on structure stability is minimal. However, instantaneous liquefaction can intensify the erosion of the seabed soil around structures. Residual liquefaction at the seabed's base adversely affects the stability of structures.

The depth of liquefaction can reach up to half the wave height [21], which will inevitably impact the stability of shoreline protective structures, as well as the coastal profile. Subsequently, an assessment of potential soil liquefaction is required as described described in [22]. The results of the current study might require recalibration based on the outcomes.

The degradation of the studied eroded shoreline segment is primarily associated with the significant alongshore sediment transport. Consequently, to mitigate these adverse effects, it is necessary to reduce the alongshore sediment flux.

A sufficient "acceleration length" is necessary to foster alongshore sediment transport, where sediments accumulate gradually. If the length of the coastline l_l, where the transport develops unobstructed significantly exceeds the width of the transport l_*, the transport reaches its full potential. However, when l_l and l_* are comparable in size, the transport lacks sufficient force. Therefore, the transport can be managed using lithodynamic barriers, such as structures that restrict the "acceleration" section. Examples of these include groynes and breakwaters.

As a potential strategy for future shoreline defense, constructing stone rubble-mound breakwaters along the coast at specific intervals could be considered. These intervals might be guided by the width of the alongshore sediment transport, indicated as l_*. For the studied construction site, l_* equals 120 meters. Given the beach's overall length of around 600 meters, spacing a pair of the breakwaters at intervals roughly equal to l_*, positioned within the potential erosion zone could be effective (Fig. 10). The length of these breakwaters could potentially correlate with the width of the sediment transport l_*, and their depth of placement could be linked to the closure depth h_* (in this case, 1.2 meters).

Another option is the use of groynes, which intercept the sediment flow in proportion to the ratio of their length l_G to the width of the flow l_*. According to [23], the distance between the groynes should not exceed 2Λ, where Λ is the structure's influence zone (eq. 9). Thus, with a groyne length of $l_G = l_*$, two groynes within the potential erosion zone would be sufficient.

Clearly, the choice of shoreline protection approach requires further justification, including economic considerations. Nonetheless, replenishing the material stock on the beach, which has significantly depleted over the past decade is a pressing task.

4. Conclusion

Based on the research findings, the following conclusions can be drawn:

– the construction of hydraulic structures within the project "Water Sports Base in the Primorsky District" will significantly reduce the rate of erosion of the "300th Anniversary Park of St. Petersburg" beach and

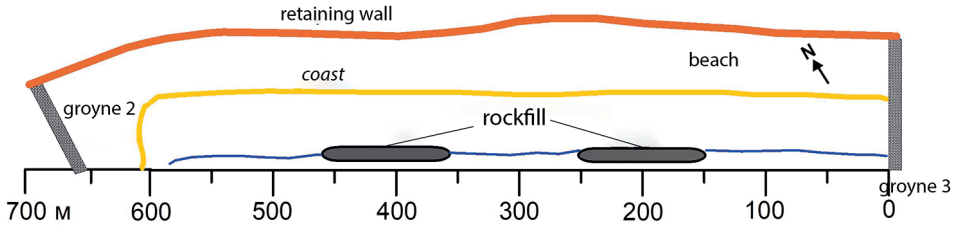

Fig. 10. One of the possible options for bank protection

decrease (limit) the erosion zone. However, the erosion process will not be completely halted. The projected timeframe for erosion of the central beach area up to the revetment wall extends up to 30 years (instead of 10 years under existing conditions).

– the construction of the mentioned structures, combined with additional measures, can stabilize the condition of the studied shoreline section of the -300th Anniversary Park of St. Petersburg".

As the primary measures for such stabilization, the following are recommended:

Constructing structures and regularly replenishing (restoring) the beach with sandy material in the central eroded zone.

Constructing structures and considering the future construction of local rubble-mound breakwaters with a length of approximately 200 meters.

References

1. Report 1290–2020.IGMI. Technical report on the results of engineering and hydrometeorological surveys. AO «Firma UNIKOM, 2020 (in Russian).
2. *Leont'ev I.O.*, *Khabidov A. Sh.* Modeling the dynamics of the coastal zone. A review of current research. P.P. Shirshov Institute of Oceanology RAS, Institute of Water and Ecological Problems SB RAS. *Novosibirsk*, *Izdatel'stvo Sibirskogo otdeleniya RAN*, 2009, 90 p. (in Russian).
3. *Hanson H.*, *Baquerizo Azofra A.*, *Falqué A.*, *Lomonaco P.*, *Payo A.* Contour–line models as tools for long–term coastal evolution. *Jornadas sobre Avances en Ingenieria Ingenieria de Costas y Oceanografia Operacional, Real Academia de Ingenieria*. 2004, 17–52. doi:10.13140/RG.2.1.4089.5524
4. *Hanson H.* GENESIS: A generalized shoreline changes numerical model. *Journal of Coastal Research*. 1989, 5(1), 1–27.
5. *Kantarzhi I.*, *Mordvintsev K.*, *Gogin A.* Numerical Analysis of the Protection of a Harbor Against Wave. *Power Technology and Engineering*. 2019, 53. doi:10.1007/s10749-019-01092-y1
6. *Leont'yev I.O.* Changes in the shoreline caused by coastal structures. *Oceanology*. 2007, 47, 877–883. doi:10.1134/S0001437007060124
7. *Badiei P.*, *Kamphuis J.W.*, *Hamilton D.G.* Physical experiments on the effects of groins on shore morphology. *24th Int. Conf. on Coastal Eng. Kobe, Japan*. 1994, 1782–1796. doi:10.1061/9780784400890.129
8. *Kantarzhi I.*, *Zheleznyak M.*, *Leont'yev I.* Modeling and monitoring of the processes in the coastal zone of Imeretinka lowland, Black Sea, Sochi. *Proceedings of Managing risks to coastal regions and communities in a changing world conference*, 2017. doi:10.31519/conferencearticle_5b1b943667afd8.23141830
9. *Baloui Y.*, *Belon R.* Evolution of Corsican pocket beaches. *Journal of Coastal Research*. 2014, 70(10070), 96–101. doi:10.2112/SI70-017.1
10. *Short A.D.*, *Masselink G.* Embayed and structurally controlled beaches. *Handbook of beach and shoreface dynamics*. *Chichester*, *England*: *John Wiley and Sons*. 1999, 392 p.
11. *Pranzini E.*, *Rosas V.*, *Jackson N.L.*, *Nordstrom K.F.* Beach changes due to sediment delivered by streams to pocket beaches during a major flood. *Geomorphology*. 2013, 199, 36–47. doi:10.1016/j.geomorph.2013.03.034
12. *Izumi N.*, *Shuto N.*, *Tanaka H.* Instability of River Mouth locations in pocket beaches. *American Society of Civil Engineers. Coast. Sed.* 1999, 628–643.
13. *Pranzini E.*, *Rosas V.* Pocket beach response to high energy e low frequency floods (Elba Island, Italy). *Journal of Coastal Research*. 2007, SI 50, 969–977.
14. *Bruun P.* The Bruun rule of erosion by sea–level rise: a discussion on large–scale two– and three–dimensional usages. *Journal of Coastal Research*. 1988, 4, 4, 627–648.
15. *Leont'yev I.O.* Changes in shoreline contour due to cross–shore structure in the sea coastal zone. *Geomorfologiya*. 2018, 3, 32–39. doi:10.7868/S0435428118030033
16. Report on research "Mathematical modeling of surges, currents, waves and bottom scouring in the Neva Bay and the mouth of the Neva River". *OOO "KARDINAL soft"*, *St. Petersburg*, 2016 (in Russian).
17. *Lappo D.D.*, *Strekalov S.S.*, *Zav'yalov V.K.* Loads and effects of wind waves on hydraulic structures. *Leningrad*, *VNII gidrotekhniki im. B.E. Vedeneeva*, 1990. 432 p. (in Russian).
18. *Leont'ev I.O.* Morphodynamic processes in the coastal zone of the sea. *Saarbrücken: LAP LAMBERT Academic Publishing*. 2014. 251 p. (in Russian).
19. Expert opinion on the construction of the facility "Water Sports Base in Primorsky District". *Vserossijskij nauchno–issledovatel'skij geologicheskij institut im. A.P. Karpinskogo*, *St. Petersburg*, 2021 (in Russian).

20. *Kuprin A.V.*, *Novakov A.D.*, *Kantarzhi I.G.*, *Gubina N.A.* Local and general scours caused by tsunami waves. *Power Technology and Engineering*. 2021, 54, 6, 836–840. doi:10.1007/s10749-021-01296-1
21. *Kuprin A.V.*, *Kantarzhi I.G.* Types of scour from tsunami waves affecting hydraulic structures. *Gidrotekhnika*. 2020, 4(61), 48–50 (in Russian).
22. *Ishihara K.*, *Yamazaki A.* Analysis of wave–induced liquefaction in seabed deposits of sand. *Soils Found*. 1984, 24 (3), 85–100. doi:10.3208/sandf1972.24.3_85
23. *Leont'yev I.O.*, *Akivis T.M.* The effect of a groin field on a sandy beach. *Oceanology*. 2020, 60(3), 412–420. doi:10.1134/S0001437020030042
24. *Leont'yev I.O.* Evaluation of depth of closure on a sandy coast. *Oceanology*. 2022, 62(2), 258–264. doi:10.1134/S0001437022020102

Литература

1. Отчет 1290–2020.ИГМИ. Технический отчет по результатам инженерно–гидрометеорологических изысканий. АО «Фирма УНИКОМ, 2020.
2. *Леонтьев И.О.*, *Хабидов А.Ш.* Моделирование динамики береговой зоны. Обзор современных исследований. Институт океанологии им. П.П. Ширшова РАН, Институт водных и экологических проблем СО РАН. Новосибирск: Издательство Сибирского отделения РАН, 2009. 90 с.
3. *Hanson H.*, *Baquerizo Azofra A.*, *Falqué A.*, *Lomonaco P.*, *Payo A.* Contour–line models as tools for long–term coastal evolution // Jornadas sobre Avances en Ingenieria Ingenieria de Costas y Oceanografia Operacional, Real Academia de Ingenieria. 2004. P. 17–52. doi:10.13140/RG.2.1.4089.5524
4. *Hanson H.* GENESIS: a generalized shoreline changes numerical model // Journal of Coastal Research. 1989. Vol. 5, No. 1. P. 1–27.
5. *Kantarzhi I.*, *Mordvintsev K.*, *Gogin A.* Numerical analysis of the protection of a harbor against waves // Power Technology and Engineering. 2019. Vol. 53. doi:10.1007/s10749-019-01092-y1
6. *Леонтьев И.О.* Изменения береговой линии моря в условиях влияния гидротехнических сооружений // Океанология. 2007. Т. 47, № 2. С. 940–946.
7. *Badiei P.*, *Kamphuis J.W.*, *Hamilton D.G.* Physical experiments on the effects of groins on shore morphology // 24th Int. Conf. on Coastal Eng. Kobe, Japan. 1994. P. 1782–1796. doi:10.1061/9780784400890.129
8. *Kantarzhi I.*, *Zheleznyak M.*, *Leont'yev I.* Modeling and monitoring of the processes in the coastal zone of Imeretinka lowland, black sea, Sochi // Proceedings of Managing risks to coastal regions and communities in a changing world conference. 2017. doi:10.31519/conferencearticle_5b1b943667afd8.23141830
9. *Baloui Y.*, *Belon R.* Evolution of Corsican pocket beaches // Journal of Coastal Research. 2014. Vol. 70, No. 10070. P. 96–101. doi:10.2112/SI70-017.1
10. *Short A.D.*, *Masselink G.* Embayed and structurally controlled beaches // Handbook of beach and shoreface dynamics. Chichester, England: John Wiley and Sons. 1999. 392 p.
11. *Pranzini E.*, *Rosas V.*, *Jackson N.L.*, *Nordstrom K.F.* Beach changes due to sediment delivered by streams to pocket beaches during a major flood // Geomorphology. 2013. Vol. 199. P. 36–47. doi:10.1016/j.geomorph.2013.03.034
12. *Izumi N.*, *Shuto N.*, *Tanaka H.* Instability of River Mouth locations in pocket beaches // American Society of Civil Engineers. Coast. Sed. 1999. P. 628–643.
13. *Pranzini E.*, *Rosas V.* Pocket beach response to high energy e low frequency floods (Elba Island, Italy) // Journal of Coastal Research. 2007. SI 50. P. 969–977.
14. *Bruun P.* The Bruun rule of erosion by sea–level rise: a discussion on large–scale two– and three–dimensional usages // Journal of Coastal Research. 1988. Vol. 4, No. 4. P. 627–648.
15. *Леонтьев И.О.* Изменения контура берега, вызванные поперечным сооружением в береговой зоне моря // Геоморфология. 2018. № 3. С. 32–39. doi:10.7868/S0435428118030033
16. Отчет о НИР «Математическое моделирование нагонов, течений, волнения и размывов дна в Невской губе и устье реки Невы». Санкт-Петербург: ООО «КАРДИНАЛ софт», 2016.
17. *Лаппо Д.Д.*, *Стрекалов С.С.*, *Завьялов В.К.* Нагрузки и воздействия ветровых волн на гидротехнические сооружения. Ленинград: ВНИИ гидротехники им. Б.Е. Веденеева, 1990. 432 с.
18. *Леонтьев И.О.* Морфодинамические процессы в береговой зоне моря. Saarbrücken: LAP LAMBERT Academic Publishing, 2014. 251 с.
19. ФГБУ «ВСЕГЕИ» Экспертное мнение по строительству объекта «База водных видов спорта в Приморском районе». Санкт-Петербург, 2021.
20. *Kuprin A.V.*, *Novakov A.D.*, *Kantarzhi I.G.*, *Gubina N.A.* Local and general scours caused by tsunami waves // Power Technology and Engineering. 2021. Vol. 54, No. 6. P. 836–840. doi:10.1007/s10749-021-01296-1

21. *Куприн А.В.*, *Кантаржи И.Г.* Типы размывов от волн цунами, воздействующих на гидротехнические сооружения // Гидротехника. 2020, № 4(61). С. 48–50.
22. *Ishihara K.*, *Yamazaki A.* Analysis of wave–induced liquefaction in seabed deposits of sand // Soils Found. 1984. Vol. 24, No 3. P. 85–100. doi:10.3208/sandf1972.24.3_85
23. *Леонтьев И.О.*, *Акивис Т.М.* О воздействии системы бун на песчаный берег // Океанология. 2020. Т. 60, № 3. С. 474–484. doi:10.31857/S0030157420030041
24. *Леонтьев И.О.* К определению глубины замыкания у песчаного берега // Океанология. 2022. Т. 62, № 2. С. 301–308. doi:10.31857/S0030157422020101

About the Authors

KANTARZHI, Izmail G., РИНЦ Author ID: 1086368, ORCID ID: 0000-0002-0587-4722, Scopus Author ID: 6602848417, 57200265787, WoS Researcher ID: A-1922–2014, kantardgi@yandex.ru

LEONT`EV, Igor O., РИНЦ Author ID: 58658, ORCID ID: 0000-0002-5010-6239, Scopus Author ID: 6603383591, WoS Researcher ID: R-8051–2016, igor.leontiev@gmail.com

KUPRIN, Alexander V., РИНЦ Author ID: 1101401, ORCID ID: 0000-0002-4186–2753, Scopus Author ID: 57222865129, rtyter55@gmail.com